

Theoretical Isochrones with Extinction in the K Band. II. $J - K$ versus K

Sungsoo S. Kim¹, Donald F. Figer², and Myung Gyoon Lee³

ABSTRACT

We calculate theoretical isochrones in a consistent way for five filter pairs near the J and K band atmospheric windows ($J-K$, $J-K'$, $J-K_s$, F110W–F205W, and F110W–F222M) using the Padova stellar evolutionary models of Girardi et al. We present magnitude transformations between various K -band filters as a function of color. Isochrones with extinction of up to 6 mag in the K band are also presented. As found for the filter pairs composed of H & K band filters, we find that the reddened isochrones of different filter pairs behave as if they follow different extinction laws, and that the extinction curves of *Hubble Space Telescope* NICMOS filter pairs in the color-magnitude diagram are considerably nonlinear. Because of these problems, extinction values estimated with NICMOS filters can be in error by up to 1.3 mag. Our calculation suggests that the extinction law implied by the observations of Rieke et al for wavelengths between the J and K bands is better described by a power-law function with an exponent of 1.66 instead of 1.59, which is commonly used with an assumption that the transmission functions of J and K filters are Dirac delta functions.

Subject headings: Hertzsprung-Russell diagram — techniques: photometric — stars: fundamental parameters — infrared: stars

1. INTRODUCTION

Kim et al. (2005, hereafter Paper I) have calculated theoretical isochrones with extinction for some H and K band filters using the Padova stellar evolutionary models by Girardi et al. (2002). In Paper I, we found that the reddened isochrones of different filter pairs in H and K bands behave as if they follow different extinction laws, and that care is needed when applying an extinction

¹Department of Astronomy and Space Science, Kyung Hee University, Yongin-shi, Kyungki-do 449-701, South Korea; sungsoo.kim@khu.ac.kr.

²Space Telescope Science Institute, 3700 San Martin Drive, Baltimore, MD 21218; figer@stsci.edu.

³Astronomy Program, SEES, Seoul National University, Seoul 151-742, South Korea; mglee@astrog.snu.ac.kr.

law obtained with one filter pair to other, similar filter pairs. For example, if the extinction law for the Johnson-Glass H and K filters obtained by Rieke, Rieke, & Paul (1989) is directly applied to the photometry from the *Hubble Space Telescope* (*HST*) NICMOS filters (F160W, F205W, and F222M), estimated extinction values can be in error by up to 0.3 mag for true extinction at K of 6 mag or less. To reduce this error, Paper I introduced an “effective extinction slope” for each filter pair and isochrone model. It was also found that the extinction behavior of isochrones in the color-magnitude diagram (CMD) for filter pair F160W–F222M is highly nonlinear (i.e., the amount of extinction is not proportional to color excess) because of a significant width difference in the two filters.

These problems are certainly not limited to the isochrones for filter pairs in the H and K bands. This problem will apply to any situation in which one applies an extinction law deduced from one filter pair to other similar filter pairs. Furthermore, the nonlinear behavior of the extinction vector in the CMD will be problematic for filter pairs with significant difference in width. In the present paper, we extend the calculations performed in Paper I to the isochrones for filter pairs in the J and K bands. The filters considered here are the four ground-based filters J , K (Johnson et al. 1966), K' (Wainscoat & Cowie 1992), and K_s (K -short; developed by M. Skrutskie; see the appendix of Persson et al. 1998), and the three NICMOS filters F110W, F205W, and F222M (transmission functions of these filters are shown in Figure 1). Out of these seven filters, we consider five filter pairs: J – K , J – K' , J – K_s , F110W–F205W, and F110W–F222M.

We adopt a Vega-based photometric system (VEGAMAG system), which uses Vega (α Lyr) as the calibrating star. For photometric zero points of NICMOS filters, we adopt $\langle f_{\nu}^{\text{Vega}} \rangle$ values from the NICMOS Data Handbook (ver. 5.0): 1775 Jy for F110W, 703.6 Jy for F205W, and 610.4 Jy for F222M. For the spectra of synthetic stellar atmospheres, we adopt Kurucz ATLAS9 no-overshoot models¹ (Kurucz 1993) calculated by Castelli et al. (1997). The metallicities of these models cover the values of $[M/H] = -2.5$ to $+0.5$. A microturbulent velocity $\xi = 2 \text{ km s}^{-1}$ and a mixing length parameter $\alpha = 1.25$ are adopted in the present study. For the temporal evolution of effective temperature and luminosity as functions of stellar mass (i.e., stellar evolutionary tracks), we adopt the “basic set” of the Padova models² (Girardi et al. 2002). We consider isochrones with a metallicity $Z = 0.0001, 0.001, 0.019$, and 0.03 . The stellar spectral library and the evolutionary tracks we adopted assume a solar chemical ratios.

For more details on the magnitude system, stellar spectral library, and evolutionary tracks that we adopt here, readers are referred to Paper I.

Throughout this paper, we generically refer to the atmospheric wavebands centered near 1.25, 1.65, and $2.2 \mu\text{m}$, as the J , H , and K bands, whereas we refer to the Johnson-Glass filters (Johnson et al. 1966; Glass 1974) as the J , H , and K filters.

¹See NOVER files at <http://kurucz.harvard.edu/grids.html>.

²See <http://pleiadi.pd.astro.it>.

2. Isochrones

We first prepare a table of magnitudes for all spectra in ATLAS9 models in the J and K band filters, covering a large range in T_{eff} , $\log g$, and $[M/H]$, using equations (5) and (6) of Paper I. We use this table as a set of interpolates for the T_{eff} , $\log g$, and Z values predicted by the stellar evolution models for a given age in order to estimate synthetic isochrones.

Isochrones for $A_\lambda = 0$, calculated in this way, are shown in Figures 2–5 for four different metallicities and four ages. The color differences between filters are more prominent for the highest metallicity isochrones. In most cases, isochrones for K' and K_s are nearly indistinguishable, and those for F205W and F222M are quite close to each other. In general, for red giants, intrinsic color differences between the atmospheric and NICMOS filters are 0.2–0.4 mag.

As an independent check of our procedure, in Figure 6 we compare our $J - K$ versus K isochrones to those calculated by Girardi et al. (2002). The isochrones match nicely, except at the extremes. The discrepancy in the bright end is caused from the empirical M giant spectra that Girardi et al. (2002) added to their spectral library, and that in the faint end is by the addition of late M dwarf spectra. The discrepancies are considerable only at the top and bottom ~ 1 mag of the isochrone, where only a small fraction of giants reside, or else stars are too faint for most observational situations.

Magnitude transformations between K -band filters can be obtained from our isochrones. We find that the magnitude difference can be well fitted by a third-order polynomial for $K < 4$ mag, and by a separate second-order polynomial for $K > 4$ mag. The largest residuals from the fit are 0.012 mag for the former and 0.008 mag for the latter. The coefficients of the best-fit functions are presented in Tables 1 and 2, along with the residuals and fitting ranges. One useful way of using these tables would be to compare the magnitudes of helium-burning clump giant stars, which are rather insensitive to metallicity or age and are often used as distance indicators, observed with different photometric systems (the clump stars show a small variation with age, however; see Figer et al. 2004).

We present here isochrones with K -band extinctions of up to 6 mag, some of which are shown in Figures 7–11. For the extinction between the J and K bands, we adopt a power law,

$$A_\lambda = A_0 \left(\frac{\lambda}{\lambda_0} \right)^{-\alpha}, \quad (1)$$

where we choose $\lambda_0 = 2.2 \mu\text{m}$, and A_0 is the extinction at λ_0 . When assuming that the transmission functions of the J and K filters are Dirac delta functions centered at 1.24 and 2.21 μm , respectively, the extinction law by Rieke et al. (1989) gives $\alpha = 1.59$. However, as discussed below in this section, the apparent extinction behavior of isochrones in the CMD can differ from the actual extinction law, as a result of a nonzero width and asymmetry of the filter transmission functions. We find that $\alpha = 1.66$ makes the isochrone for the $Z = 0.019$, age = 10^9 yr model behave in the CMD as if it followed an extinction law with $\alpha = 1.59$. We choose this particular isochrone for calibrating

the extinction law, with the assumption that the stars used in Rieke et al. (1989) to derive their extinction law, which are the stars in the central parsec of our Galaxy, can be represented by the same metallicity and age. For the sake of comparison, isochrones in Figures 7–11 have been dereddened by the amount $A_0(\lambda_c/\lambda_0)^{-1.66}$, where the central wavelength of the filter λ_c is defined by equation (8) of Paper I, and given in Table 3.

Since we have dereddened the isochrones with the known amount of extinction at λ_c , all the dereddened isochrones with different extinction values in Figures 7–11 should be coincident if the filter transmission functions were Dirac delta functions centered at λ_c . As in Paper I, the dereddened isochrones misalign significantly, and this implies that the amount of extinction inferred from a CMD is sensitively dependent on the shape of the filter transmission function.

When estimating the amount of extinction from an observed CMD, one converts an observed color excess to an extinction value, following an assumed extinction law, which usually has the form of a power law. When one has photometric data from a pair of two filters, X and Y , the amount of extinction can be estimated by

$$\begin{aligned} A_Y^{est} &= \frac{(m_X - m_Y) - (m_X - m_Y)_0}{A_X/A_Y - 1} \\ &= \frac{(m_X - m_Y) - (m_X - m_Y)_0}{(\lambda_X/\lambda_Y)^{-\alpha} - 1}, \end{aligned} \quad (2)$$

where m_X , m_Y and λ_X , λ_Y are the magnitudes and the central wavelengths of the two filters, respectively, and subscript 0 denotes the intrinsic value. For estimating extinction from our isochrones, we first use $\alpha = 1.59$. Figure 12 shows the difference between the inferred extinction values, using equation (2) and colors from our reddened isochrones, and the actual extinction values. Here the extinction of each isochrone has been calculated using the mean color (for A_Y^{est}) and magnitude (for A_Y) of the reddened isochrone data points having intrinsic K -band magnitudes between -6 and 0 mag. As the figure shows, the differences between estimated and actual extinction values are much larger for the NICMOS filter pairs. The largest relative difference is $\sim 24\%$, and the largest absolute difference is 1.25 mag. Note that the extinction estimates for the $Z = 0.019$ and age = 10^9 yr model inferred from H and K are very close to the actual extinction values, justifying our choice of $\alpha = 1.66$ for equation (1). The error bar in the figure represents the standard deviation of $A_Y^{est} - A_Y$ values. Some of the F110W isochrones show quite large deviations, as pointed out in Appendix A of Lee et al. (2001).

To reduce the problems seen in Figure 12, Paper I introduced an “effective extinction slope” α_{eff} for each filter pair and isochrone model, which is defined such that it better describes the extinction behavior in the CMD:

$$\alpha_{eff} = -\frac{\log(1 + 1/b)}{\log(\lambda_X/\lambda_Y)}, \quad (3)$$

where b is the slope of the straight line that fits the distribution of reddened magnitudes versus reddened colors, as in Figure 13. This figure shows reddened K -band magnitudes and colors for the $Z = 0.019$ and age = 10^9 yr isochrone (the figure only shows an isochrone data point whose

intrinsic K magnitude is 0, as an example). We calculate b for data points of each isochrone whose intrinsic K magnitudes are between -6 and 0 mag, and take an average for each isochrone model. Table 4 shows the averages and standard deviations of α_{eff} values for each isochrone model. For atmospheric filters, the standard deviations of α_{eff} in an isochrone is generally much smaller than the differences of average α_{eff} values between different isochrones, while those for NICMOS filters are relatively larger. The average α_{eff} values range from 1.403 to 1.610, which are 15% to 0.02% smaller than the original α value we adopted for extinction, 1.66. As seen in Figure 14, extinction values estimated by equation (2) with α_{eff} are closer to the actual values for atmospheric filters, but still deviate significantly from the actual values for NICMOS filters, because of the nonlinear extinction seen in Figure 13.

As pointed out in Paper I, the nonlinear extinction behavior of NICMOS filters is due to a significant difference in relative widths of the two filters: the width to central wavelength ratio $\Delta\lambda/\lambda_c$ is ~ 0.5 for F110W, while those for F205W and F222M are ~ 0.3 and ~ 0.07 , respectively. Figure 15 shows the effect of the filter width by comparing the extinction behavior of six imaginary filter pairs. Filter pair a represents J and K , whose $\Delta\lambda/\lambda_c$ values are both ~ 0.16 , and its extinction behavior in the CMD is nearly linear. On the other hand, filter pairs b and c , which represent filter pairs F110W–F205W and F110W–F222M, show considerable nonlinearity. When the $\Delta\lambda/\lambda_c$ of the short-wavelength filter is reduced by $\sim 60\%$, however, the extinction behaves much more linearly (d and e). This shows that the nonlinear extinction in filter pairs F110W–F205W and F110W–F222M is due to a relatively larger $\Delta\lambda/\lambda_c$ value of the F110W filter. When both filters have the same large $\Delta\lambda/\lambda_c$ values (~ 0.5), the extinction becomes almost linear again (f).

The introduction of effective extinction slopes does not alleviate the nonlinear extinction problem of NICMOS filter pairs. So in Table 5 we provide the coefficients of best-fit third-order polynomials of the extinction curves for NICMOS filter pairs shown in Figure 12 so that one can accurately estimate the extinction value for NICMOS filter pairs as well. Note that we assumed $\alpha = 1.59$ for all isochrone models when estimating A_Y^{est} in Figure 12.

As in paper I, we find that for the filters whose extinction behavior is relatively linear, the transformation of extinction values from filter Y to filter Y' can be obtained by

$$A_{Y'} = A_Y \left(\frac{\lambda_{Y'}}{\lambda_Y} \right)^{-\alpha}, \quad (4)$$

if A_Y is estimated with α_{eff} , and the original α value of 1.66 is used in the above equation.

3. SUMMARY

We have calculated in a consistent way five near-infrared theoretical isochrones for filter pairs composed of J and K filters: J – K , J – K' , J – K_s , F110W–F205W, and F110W–F222M. We presented isochrones for a Z of 0.0001–0.03 and an age of 10^7 – 10^{10} yr. Even in the same Vega magnitude system, near-infrared colors of the same isochrone can be different by up to ~ 0.4 mag at the

bright end of the isochrone for different filter pairs. The difference in intrinsic colors for a red giant for atmospheric filters and the *HST* NICMOS filters is generally 0.2–0.4 mag. We have provided magnitude transformations between *K*-band filters as a function of color from *J* and *K* band filters. We also presented isochrones with A_K of up to 6 mag. We found that care is needed when comparing extinction values that are estimated using different filter pairs, in particular when comparing those of atmospheric and NICMOS filter pairs: extinction values inferred using NICMOS filters can be in error by up to 1.3 mag. To alleviate this problem, we introduced an “effective extinction slope” for each filter pair and isochrone model, which describes the extinction-dependent behavior of isochrones in the observed CMD. We also provided a procedure to accurately estimate the extinction value for NICMOS filter pairs, whose extinction curves in the CMD are highly nonlinear.

We thank Jae-Woo Lee for a helpful discussion. S. S. K. was supported by the Astrophysical Research Center for the Structure and Evolution of the Cosmos (ARCSEC) of the Korea Science and Engineering Foundation through the Science Research Center (SRC) program. M. G. L. was in part supported by the ABRL (R14-2002-058-01000-0) and the BK21 program.

REFERENCES

- Castelli, F., Gratton, R. G., & Kurucz, R. L. 1997, *A&A*, 318, 841
- Figer, D. F., Rich, R. M., Kim, S. S., Morris, M., & Serabyn, E. 2004, *ApJ*, 601, 319
- Girardi, L., Bertelli, G., Bressan, A., Chiosi, C., Groenewegen, M. A. T., Marigo, P., Salsasnich, B., & Weiss, A. 2002, *A&A*, 391, 195
- Glass, I. S. 1974, *Mon. Notes Astr. Soc. Sth. Afr.*, 33, 53
- Johnson, H. L., Iriarte, B., Mitchell, R. I., & Wisniewskj, W. Z. 1966, *Comm. Lunar Plan. Lab.*, 4, 99
- Kim, S. S., Figer, D. F., Lee, M. G., & Oh, S. 2005, *PASP*, 117, 445 (Paper I)
- Kurucz, R. L. 1993, in *The Stellar Populations of Galaxies*, eds. B. Barbuy, & A. Renzini, (Dordrecht, Kluwer), *IAU Symp.*, 149, 225
- Lee, J.-W., Carney, B. W., Fullton, L. K., & Stetson, P. B. 2001, *AJ*, 122, 3136
- Persson, S. E., Murphy, D. C., Krzeminski, W., Roth, M., & Rieke, M. J. 1998, *AJ*, 116, 2475
- Rieke, G. H., Rieke, M. J., & Paul, A. E. 1989, *ApJ*, 336, 752
- Wainscoat, R. J., & Cowie, L. L. 1992, *AJ*, 103, 332

Table 1. Best-Fit Coefficients for Magnitude Differences ($K < 4$ mag)

Color	Magnitude Difference	Z	c_0	c_1	c_2	c_3	Residual ^a (mag)	Fitting Range ^b (mag \sim mag)
$J - K$	$K' - K$	0.0001	-0.001	0.028	-0.064	0.057	0.004	-0.236 \sim 0.720
$J - K$	$K' - K$	0.001	-0.001	0.032	-0.039	-0.036	0.007	-0.162 \sim 0.859
$J - K$	$K' - K$	0.019	0.002	0.036	-0.147	0.074	0.011	-0.213 \sim 1.250
$J - K$	$K' - K$	0.03	0.001	0.042	-0.163	0.083	0.007	-0.129 \sim 1.237
$J - K$	$K_s - K$	0.0001	-0.000	0.012	-0.013	0.006	0.002	-0.236 \sim 0.720
$J - K$	$K_s - K$	0.001	-0.000	0.015	-0.003	-0.052	0.006	-0.162 \sim 0.859
$J - K$	$K_s - K$	0.019	0.002	0.017	-0.103	0.051	0.009	-0.213 \sim 1.250
$J - K$	$K_s - K$	0.03	0.001	0.024	-0.121	0.061	0.006	-0.129 \sim 1.237
$J - K$	F205W- K	0.0001	-0.030	0.052	-0.143	0.150	0.006	-0.236 \sim 0.720
$J - K$	F205W- K	0.001	-0.030	0.056	-0.095	0.028	0.005	-0.162 \sim 0.859
$J - K$	F205W- K	0.019	-0.029	0.060	-0.147	0.074	0.007	-0.213 \sim 1.250
$J - K$	F205W- K	0.03	-0.029	0.061	-0.147	0.077	0.004	-0.129 \sim 1.237
$J - K$	F222M- K	0.0001	-0.031	-0.002	-0.001	-0.019	0.005	-0.236 \sim 0.720
$J - K$	F222M- K	0.001	-0.030	0.001	-0.010	-0.046	0.006	-0.162 \sim 0.859
$J - K$	F222M- K	0.019	-0.028	0.002	-0.113	0.060	0.012	-0.213 \sim 1.250
$J - K$	F222M- K	0.03	-0.028	0.009	-0.134	0.071	0.007	-0.129 \sim 1.237
$J - K'$	$K - K'$	0.0001	0.001	-0.029	0.068	-0.061	0.004	-0.224 \sim 0.715
$J - K'$	$K - K'$	0.001	0.001	-0.033	0.047	0.024	0.006	-0.155 \sim 0.881
$J - K'$	$K - K'$	0.019	-0.001	-0.037	0.142	-0.070	0.011	-0.203 \sim 1.290
$J - K'$	$K - K'$	0.03	-0.001	-0.042	0.154	-0.076	0.006	-0.123 \sim 1.278
$J - K'$	$K_s - K'$	0.0001	0.001	-0.017	0.054	-0.055	0.003	-0.224 \sim 0.715
$J - K'$	$K_s - K'$	0.001	0.001	-0.018	0.038	-0.017	0.002	-0.155 \sim 0.881
$J - K'$	$K_s - K'$	0.019	0.000	-0.019	0.043	-0.022	0.003	-0.203 \sim 1.290
$J - K'$	$K_s - K'$	0.03	0.001	-0.019	0.040	-0.021	0.002	-0.123 \sim 1.278
$J - K'$	F205W- K'	0.0001	-0.029	0.025	-0.085	0.099	0.003	-0.224 \sim 0.715
$J - K'$	F205W- K'	0.001	-0.029	0.024	-0.054	0.058	0.004	-0.155 \sim 0.881
$J - K'$	F205W- K'	0.019	-0.031	0.024	-0.002	0.001	0.005	-0.203 \sim 1.290
$J - K'$	F205W- K'	0.03	-0.030	0.019	0.012	-0.004	0.005	-0.123 \sim 1.278
$J - K'$	F222M- K'	0.0001	-0.030	-0.032	0.067	-0.080	0.005	-0.224 \sim 0.715
$J - K'$	F222M- K'	0.001	-0.029	-0.032	0.032	-0.012	0.003	-0.155 \sim 0.881
$J - K'$	F222M- K'	0.019	-0.030	-0.035	0.036	-0.015	0.004	-0.203 \sim 1.290
$J - K'$	F222M- K'	0.03	-0.029	-0.035	0.031	-0.013	0.003	-0.123 \sim 1.278
$J - K_s$	$K - K_s$	0.0001	0.000	-0.012	0.013	-0.005	0.002	-0.232 \sim 0.718
$J - K_s$	$K - K_s$	0.001	0.000	-0.015	0.008	0.043	0.006	-0.160 \sim 0.879
$J - K_s$	$K - K_s$	0.019	-0.002	-0.017	0.098	-0.047	0.009	-0.209 \sim 1.289
$J - K_s$	$K - K_s$	0.03	-0.001	-0.023	0.113	-0.055	0.006	-0.127 \sim 1.278
$J - K_s$	$K' - K_s$	0.0001	-0.001	0.017	-0.052	0.053	0.003	-0.232 \sim 0.718
$J - K_s$	$K' - K_s$	0.001	-0.001	0.018	-0.037	0.017	0.002	-0.160 \sim 0.879
$J - K_s$	$K' - K_s$	0.019	-0.000	0.019	-0.042	0.022	0.003	-0.209 \sim 1.289
$J - K_s$	$K' - K_s$	0.03	-0.001	0.018	-0.039	0.021	0.002	-0.127 \sim 1.278
$J - K_s$	F205W- K_s	0.0001	-0.029	0.041	-0.133	0.147	0.005	-0.232 \sim 0.718
$J - K_s$	F205W- K_s	0.001	-0.030	0.042	-0.090	0.075	0.004	-0.160 \sim 0.879
$J - K_s$	F205W- K_s	0.019	-0.031	0.042	-0.044	0.022	0.006	-0.209 \sim 1.289
$J - K_s$	F205W- K_s	0.03	-0.031	0.037	-0.027	0.016	0.005	-0.127 \sim 1.278
$J - K_s$	F222M- K_s	0.0001	-0.030	-0.014	0.012	-0.024	0.005	-0.232 \sim 0.718

Table 1—Continued

Color	Magnitude Difference	Z	c_0	c_1	c_2	c_3	Residual ^a (mag)	Fitting Range ^b (mag ~ mag)
$J - K_s$	F222M– K_s	0.001	–0.030	–0.014	–0.007	0.006	0.004	–0.160 ~ 0.879
$J - K_s$	F222M– K_s	0.019	–0.030	–0.016	–0.008	0.008	0.005	–0.209 ~ 1.289
$J - K_s$	F222M– K_s	0.03	–0.030	–0.016	–0.010	0.008	0.004	–0.127 ~ 1.278
F110W–F205W	$K - F205W$	0.0001	0.030	–0.040	0.085	–0.070	0.007	–0.304 ~ 0.928
F110W–F205W	$K - F205W$	0.001	0.030	–0.043	0.053	–0.010	0.005	–0.210 ~ 1.122
F110W–F205W	$K - F205W$	0.019	0.029	–0.047	0.086	–0.033	0.006	–0.272 ~ 1.621
F110W–F205W	$K - F205W$	0.03	0.029	–0.047	0.086	–0.034	0.004	–0.166 ~ 1.615
F110W–F205W	$K' - F205W$	0.0001	0.029	–0.018	0.048	–0.043	0.003	–0.304 ~ 0.928
F110W–F205W	$K' - F205W$	0.001	0.029	–0.018	0.035	–0.030	0.003	–0.210 ~ 1.122
F110W–F205W	$K' - F205W$	0.019	0.031	–0.017	–0.000	–0.000	0.005	–0.272 ~ 1.621
F110W–F205W	$K' - F205W$	0.03	0.030	–0.013	–0.010	0.003	0.005	–0.166 ~ 1.615
F110W–F205W	$K_s - F205W$	0.0001	0.029	–0.031	0.078	–0.067	0.005	–0.304 ~ 0.928
F110W–F205W	$K_s - F205W$	0.001	0.030	–0.032	0.055	–0.036	0.004	–0.210 ~ 1.122
F110W–F205W	$K_s - F205W$	0.019	0.031	–0.032	0.026	–0.011	0.006	–0.272 ~ 1.621
F110W–F205W	$K_s - F205W$	0.03	0.031	–0.027	0.014	–0.007	0.005	–0.166 ~ 1.615
F110W–F205W	F222M–F205W	0.0001	–0.001	–0.041	0.085	–0.079	0.007	–0.304 ~ 0.928
F110W–F205W	F222M–F205W	0.001	–0.000	–0.042	0.050	–0.033	0.004	–0.210 ~ 1.122
F110W–F205W	F222M–F205W	0.019	0.001	–0.043	0.018	–0.006	0.006	–0.272 ~ 1.621
F110W–F205W	F222M–F205W	0.03	0.001	–0.037	0.005	–0.002	0.004	–0.166 ~ 1.615
F110W–F222M	$K - F222M$	0.0001	0.031	0.001	0.001	0.008	0.005	–0.324 ~ 0.955
F110W–F222M	$K - F222M$	0.001	0.030	–0.001	0.004	0.021	0.005	–0.222 ~ 1.152
F110W–F222M	$K - F222M$	0.019	0.028	–0.003	0.063	–0.024	0.011	–0.291 ~ 1.665
F110W–F222M	$K - F222M$	0.03	0.028	–0.009	0.076	–0.029	0.006	–0.176 ~ 1.669
F110W–F222M	$K' - F222M$	0.0001	0.030	0.021	–0.033	0.032	0.005	–0.324 ~ 0.955
F110W–F222M	$K' - F222M$	0.001	0.029	0.022	–0.013	0.003	0.003	–0.222 ~ 1.152
F110W–F222M	$K' - F222M$	0.019	0.030	0.024	–0.017	0.005	0.004	–0.291 ~ 1.665
F110W–F222M	$K' - F222M$	0.03	0.029	0.024	–0.014	0.004	0.003	–0.176 ~ 1.669
F110W–F222M	$K_s - F222M$	0.0001	0.030	0.010	–0.006	0.011	0.005	–0.324 ~ 0.955
F110W–F222M	$K_s - F222M$	0.001	0.030	0.009	0.005	–0.003	0.004	–0.222 ~ 1.152
F110W–F222M	$K_s - F222M$	0.019	0.030	0.011	0.007	–0.004	0.005	–0.291 ~ 1.665
F110W–F222M	$K_s - F222M$	0.03	0.030	0.010	0.009	–0.005	0.004	–0.176 ~ 1.669
F110W–F222M	F205W–F222M	0.0001	0.001	0.038	–0.076	0.070	0.007	–0.324 ~ 0.955
F110W–F222M	F205W–F222M	0.001	0.000	0.040	–0.045	0.030	0.004	–0.222 ~ 1.152
F110W–F222M	F205W–F222M	0.019	–0.001	0.041	–0.017	0.005	0.006	–0.291 ~ 1.665
F110W–F222M	F205W–F222M	0.03	–0.001	0.036	–0.004	0.002	0.004	–0.176 ~ 1.669

Note. — Magnitude differences are fitted to a function $[\text{Mag Diff}] = c_0 + c_1[\text{Color}] + c_2[\text{Color}]^2 + c_3[\text{Color}]^3$. Only the data points that have $\log T_{\text{eff}} \geq 3500$ K and $\log g \geq 0$ were considered for the fitting.

^aThe largest absolute residual.

^bColor range where the fit is valid.

Table 2. Best-Fit Coefficients for Magnitude Differences ($K > 4$ mag)

Color	Magnitude Difference	Z	c_0	c_1	c_2	Residual ^a (mag)	Fitting Range ^b (mag \sim mag)
$J - K$	$K' - K$	0.0001	-0.012	0.047	-0.003	0.001	0.332 \sim 0.772
$J - K$	$K' - K$	0.001	0.034	-0.126	0.127	0.003	0.338 \sim 0.893
$J - K$	$K' - K$	0.019	0.102	-0.331	0.252	0.004	0.539 \sim 0.992
$J - K$	$K' - K$	0.03	0.129	-0.401	0.291	0.003	0.559 \sim 0.987
$J - K$	$K_s - K$	0.0001	-0.010	0.042	-0.019	0.001	0.332 \sim 0.772
$J - K$	$K_s - K$	0.001	0.018	-0.059	0.055	0.002	0.338 \sim 0.893
$J - K$	$K_s - K$	0.019	0.055	-0.182	0.134	0.003	0.539 \sim 0.992
$J - K$	$K_s - K$	0.03	0.073	-0.229	0.160	0.002	0.559 \sim 0.987
$J - K$	F205W- K	0.0001	-0.049	0.082	0.000	0.001	0.332 \sim 0.772
$J - K$	F205W- K	0.001	0.026	-0.203	0.217	0.004	0.338 \sim 0.893
$J - K$	F205W- K	0.019	0.127	-0.490	0.386	0.007	0.539 \sim 0.992
$J - K$	F205W- K	0.03	0.173	-0.601	0.447	0.004	0.559 \sim 0.987
$J - K$	F222M- K	0.0001	-0.026	-0.023	0.003	0.001	0.332 \sim 0.772
$J - K$	F222M- K	0.001	-0.027	-0.016	-0.007	0.001	0.338 \sim 0.893
$J - K$	F222M- K	0.019	-0.030	-0.027	0.002	0.001	0.539 \sim 0.992
$J - K$	F222M- K	0.03	-0.035	-0.020	-0.002	0.001	0.559 \sim 0.987
$J - K'$	$K - K'$	0.0001	0.012	-0.050	0.004	0.001	0.328 \sim 0.750
$J - K'$	$K - K'$	0.001	-0.037	0.138	-0.140	0.003	0.334 \sim 0.871
$J - K'$	$K - K'$	0.019	-0.127	0.401	-0.300	0.005	0.543 \sim 0.975
$J - K'$	$K - K'$	0.03	-0.174	0.520	-0.369	0.003	0.593 \sim 0.971
$J - K'$	$K_s - K'$	0.0001	0.002	-0.006	-0.017	0.001	0.328 \sim 0.750
$J - K'$	$K_s - K'$	0.001	-0.018	0.074	-0.080	0.003	0.334 \sim 0.871
$J - K'$	$K_s - K'$	0.019	-0.060	0.184	-0.143	0.002	0.543 \sim 0.975
$J - K'$	$K_s - K'$	0.03	-0.080	0.233	-0.172	0.001	0.593 \sim 0.971
$J - K'$	F205W- K'	0.0001	-0.038	0.036	0.004	0.001	0.328 \sim 0.750
$J - K'$	F205W- K'	0.001	-0.006	-0.087	0.101	0.002	0.334 \sim 0.871
$J - K'$	F205W- K'	0.019	0.040	-0.202	0.166	0.003	0.543 \sim 0.975
$J - K'$	F205W- K'	0.03	0.077	-0.286	0.211	0.002	0.593 \sim 0.971
$J - K'$	F222M- K'	0.0001	-0.013	-0.074	0.007	0.001	0.328 \sim 0.750
$J - K'$	F222M- K'	0.001	-0.065	0.125	-0.150	0.004	0.334 \sim 0.871
$J - K'$	F222M- K'	0.019	-0.160	0.383	-0.305	0.004	0.543 \sim 0.975
$J - K'$	F222M- K'	0.03	-0.214	0.513	-0.380	0.003	0.593 \sim 0.971
$J - K_s$	$K - K_s$	0.0001	0.010	-0.043	0.020	0.001	0.330 \sim 0.761
$J - K_s$	$K - K_s$	0.001	-0.018	0.060	-0.056	0.002	0.335 \sim 0.885
$J - K_s$	$K - K_s$	0.019	-0.060	0.197	-0.143	0.003	0.544 \sim 0.989
$J - K_s$	$K - K_s$	0.03	-0.084	0.257	-0.177	0.002	0.594 \sim 0.986
$J - K_s$	$K' - K_s$	0.0001	-0.002	0.006	0.016	0.001	0.330 \sim 0.761
$J - K_s$	$K' - K_s$	0.001	0.017	-0.069	0.075	0.003	0.335 \sim 0.885
$J - K_s$	$K' - K_s$	0.019	0.054	-0.165	0.128	0.002	0.544 \sim 0.989
$J - K_s$	$K' - K_s$	0.03	0.070	-0.204	0.151	0.001	0.594 \sim 0.986
$J - K_s$	F205W- K_s	0.0001	-0.040	0.042	0.019	0.001	0.330 \sim 0.761
$J - K_s$	F205W- K_s	0.001	0.010	-0.149	0.168	0.003	0.335 \sim 0.885
$J - K_s$	F205W- K_s	0.019	0.085	-0.343	0.276	0.005	0.544 \sim 0.989
$J - K_s$	F205W- K_s	0.03	0.134	-0.454	0.337	0.003	0.594 \sim 0.986
$J - K_s$	F222M- K_s	0.0001	-0.015	-0.068	0.024	0.001	0.330 \sim 0.761

Table 2—Continued

Color	Magnitude Difference	Z	c_0	c_1	c_2	Residual ^a (mag)	Fitting Range ^b (mag \sim mag)
$J - K_s$	F222M– K_s	0.001	–0.045	0.046	–0.064	0.002	0.335 \sim 0.885
$J - K_s$	F222M– K_s	0.019	–0.092	0.174	–0.144	0.003	0.544 \sim 0.989
$J - K_s$	F222M– K_s	0.03	–0.122	0.245	–0.184	0.002	0.594 \sim 0.986
F110W–F205W	$K - F205W$	0.0001	0.054	–0.071	–0.000	0.001	0.454 \sim 0.961
F110W–F205W	$K - F205W$	0.001	–0.050	0.223	–0.176	0.005	0.484 \sim 1.107
F110W–F205W	$K - F205W$	0.019	–0.162	0.460	–0.278	0.008	0.724 \sim 1.252
F110W–F205W	$K - F205W$	0.03	–0.231	0.584	–0.328	0.005	0.784 \sim 1.257
F110W–F205W	$K' - F205W$	0.0001	0.040	–0.030	–0.003	0.001	0.454 \sim 0.961
F110W–F205W	$K' - F205W$	0.001	–0.002	0.088	–0.074	0.002	0.484 \sim 1.107
F110W–F205W	$K' - F205W$	0.019	–0.036	0.150	–0.097	0.003	0.724 \sim 1.252
F110W–F205W	$K' - F205W$	0.03	–0.068	0.203	–0.118	0.002	0.784 \sim 1.257
F110W–F205W	$K_s - F205W$	0.0001	0.042	–0.033	–0.015	0.001	0.454 \sim 0.961
F110W–F205W	$K_s - F205W$	0.001	–0.026	0.162	–0.133	0.004	0.484 \sim 1.107
F110W–F205W	$K_s - F205W$	0.019	–0.095	0.291	–0.182	0.005	0.724 \sim 1.252
F110W–F205W	$K_s - F205W$	0.03	–0.141	0.370	–0.214	0.003	0.784 \sim 1.257
F110W–F205W	F222M–F205W	0.0001	0.030	–0.091	0.002	0.001	0.454 \sim 0.961
F110W–F205W	F222M–F205W	0.001	–0.079	0.218	–0.186	0.005	0.484 \sim 1.107
F110W–F205W	F222M–F205W	0.019	–0.190	0.438	–0.277	0.008	0.724 \sim 1.252
F110W–F205W	F222M–F205W	0.03	–0.266	0.569	–0.330	0.005	0.784 \sim 1.257
F110W–F222M	$K - F222M$	0.0001	0.025	0.018	–0.002	0.001	0.465 \sim 1.017
F110W–F222M	$K - F222M$	0.001	0.027	0.010	0.006	0.001	0.496 \sim 1.170
F110W–F222M	$K - F222M$	0.019	0.025	0.029	–0.005	0.001	0.742 \sim 1.322
F110W–F222M	$K - F222M$	0.03	0.031	0.023	–0.002	0.001	0.806 \sim 1.327
F110W–F222M	$K' - F222M$	0.0001	0.011	0.055	–0.003	0.001	0.465 \sim 1.017
F110W–F222M	$K' - F222M$	0.001	0.069	–0.103	0.089	0.004	0.496 \sim 1.170
F110W–F222M	$K' - F222M$	0.019	0.122	–0.208	0.131	0.004	0.742 \sim 1.322
F110W–F222M	$K' - F222M$	0.03	0.152	–0.259	0.151	0.003	0.806 \sim 1.327
F110W–F222M	$K_s - F222M$	0.0001	0.013	0.053	–0.014	0.001	0.465 \sim 1.017
F110W–F222M	$K_s - F222M$	0.001	0.048	–0.043	0.042	0.002	0.496 \sim 1.170
F110W–F222M	$K_s - F222M$	0.019	0.078	–0.103	0.068	0.003	0.742 \sim 1.322
F110W–F222M	$K_s - F222M$	0.03	0.100	–0.140	0.082	0.002	0.806 \sim 1.327
F110W–F222M	F205W–F222M	0.0001	–0.028	0.083	–0.001	0.001	0.465 \sim 1.017
F110W–F222M	F205W–F222M	0.001	0.065	–0.173	0.148	0.005	0.496 \sim 1.170
F110W–F222M	F205W–F222M	0.019	0.139	–0.313	0.200	0.006	0.742 \sim 1.322
F110W–F222M	F205W–F222M	0.03	0.195	–0.404	0.235	0.004	0.806 \sim 1.327

Note. — Magnitude differences are fitted to a function $[\text{Mag Diff}] = c_0 + c_1[\text{Color}] + c_2[\text{Color}]^2$. Only the data points that have $\log T_{eff} \geq 3500$ K and $\log g \geq 0$ were considered for the fitting.

^aThe largest absolute residual.

^bColor range where the fit is valid.

Table 3. Central Wavelength λ_c (μm)

J	K	K'	K_s	F110W	F205W	F222M
1.237	2.212	2.114	2.160	1.140	2.079	2.219

Note. — λ_c is defined by eq. (8) of Paper I.

Table 4. Averages and Standard Deviations of α_{eff} Values

Isochrone Model		$J - K$	$J - K'$	$J - K_s$	F110W–F205W	F110W–F222M
Z	Age					
0.0001	10^7	1.610 ± 0.000	1.608 ± 0.000	1.610 ± 0.000	1.479 ± 0.001	1.500 ± 0.002
0.0001	10^8	1.608 ± 0.003	1.605 ± 0.004	1.607 ± 0.004	1.467 ± 0.011	1.486 ± 0.011
0.0001	10^9	1.600 ± 0.004	1.597 ± 0.005	1.598 ± 0.004	1.440 ± 0.013	1.460 ± 0.012
0.0001	10^{10}	1.596 ± 0.003	1.593 ± 0.003	1.595 ± 0.003	1.429 ± 0.008	1.450 ± 0.007
0.001	6.3×10^7	1.608 ± 0.004	1.605 ± 0.004	1.607 ± 0.004	1.467 ± 0.012	1.487 ± 0.012
0.001	10^8	1.605 ± 0.006	1.603 ± 0.006	1.604 ± 0.006	1.459 ± 0.017	1.478 ± 0.017
0.001	10^9	1.595 ± 0.004	1.593 ± 0.003	1.595 ± 0.003	1.430 ± 0.008	1.451 ± 0.007
0.001	10^{10}	1.591 ± 0.005	1.590 ± 0.003	1.592 ± 0.003	1.421 ± 0.010	1.444 ± 0.008
0.019	10^7	1.610 ± 0.000	1.608 ± 0.000	1.610 ± 0.000	1.478 ± 0.001	1.498 ± 0.002
0.019	10^8	1.599 ± 0.011	1.599 ± 0.009	1.600 ± 0.009	1.448 ± 0.028	1.470 ± 0.025
0.019	10^9	1.588 ± 0.006	1.590 ± 0.004	1.590 ± 0.004	1.418 ± 0.012	1.442 ± 0.010
0.019	10^{10}	1.582 ± 0.005	1.586 ± 0.003	1.587 ± 0.003	1.406 ± 0.011	1.432 ± 0.009
0.03	6.3×10^7	1.606 ± 0.007	1.605 ± 0.006	1.606 ± 0.006	1.465 ± 0.019	1.485 ± 0.018
0.03	10^8	1.599 ± 0.012	1.599 ± 0.009	1.600 ± 0.010	1.448 ± 0.029	1.470 ± 0.026
0.03	10^9	1.586 ± 0.006	1.589 ± 0.004	1.590 ± 0.004	1.415 ± 0.012	1.440 ± 0.010
0.03	10^{10}	1.581 ± 0.005	1.585 ± 0.003	1.586 ± 0.003	1.403 ± 0.011	1.429 ± 0.009

Note. — Data are presented in the form of average \pm standard deviation. The average and standard deviation values are calculated from the data points of each isochrone whose intrinsic K magnitudes are between -6 and 0 mag.

Table 5. Extinction Behavior of *HST* NICMOS Filter Pairs

Isochrone Model		F110W–F205W					F110W–F222M				
<i>Z</i>	Age	<i>c</i> ₀	<i>c</i> ₁	<i>c</i> ₂	<i>c</i> ₃	$\sigma(A^{est})$	<i>c</i> ₀	<i>c</i> ₁	<i>c</i> ₂	<i>c</i> ₃	$\sigma(A^{est})$
0.0001	10 ⁷	7.07E-04	2.07E-01	−1.08E-01	7.77E-03	0.011	−9.83E-05	2.67E-01	−1.18E-01	7.01E-03	0.013
0.0001	10 ⁸	9.78E-04	1.75E-01	−1.05E-01	7.70E-03	0.077	1.18E-04	2.37E-01	−1.16E-01	7.07E-03	0.080
0.0001	10 ⁹	1.61E-03	1.14E-01	−1.00E-01	7.88E-03	0.082	6.21E-04	1.84E-01	−1.14E-01	7.41E-03	0.083
0.0001	10 ¹⁰	1.82E-03	8.93E-02	−9.82E-02	7.95E-03	0.049	7.90E-04	1.62E-01	−1.13E-01	7.53E-03	0.050
0.001	6.3 × 10 ⁷	9.79E-04	1.75E-01	−1.05E-01	7.69E-03	0.082	1.01E-04	2.38E-01	−1.16E-01	7.05E-03	0.084
0.001	10 ⁸	1.16E-03	1.58E-01	−1.04E-01	7.77E-03	0.115	2.30E-04	2.21E-01	−1.16E-01	7.17E-03	0.118
0.001	10 ⁹	1.75E-03	9.25E-02	−9.86E-02	7.93E-03	0.049	6.72E-04	1.66E-01	−1.13E-01	7.53E-03	0.047
0.001	10 ¹⁰	1.86E-03	7.52E-02	−9.74E-02	7.98E-03	0.057	8.48E-04	1.51E-01	−1.12E-01	7.57E-03	0.054
0.019	10 ⁷	7.77E-04	2.03E-01	−1.08E-01	7.74E-03	0.010	−7.16E-05	2.64E-01	−1.18E-01	7.01E-03	0.011
0.019	10 ⁸	1.33E-03	1.36E-01	−1.02E-01	7.82E-03	0.172	3.57E-04	2.05E-01	−1.15E-01	7.23E-03	0.171
0.019	10 ⁹	1.93E-03	6.95E-02	−9.71E-02	7.97E-03	0.068	8.10E-04	1.46E-01	−1.12E-01	7.55E-03	0.066
0.019	10 ¹⁰	2.07E-03	4.13E-02	−9.42E-02	7.93E-03	0.064	8.75E-04	1.22E-01	−1.09E-01	7.48E-03	0.062
0.03	6.3 × 10 ⁷	1.03E-03	1.72E-01	−1.05E-01	7.73E-03	0.120	1.43E-04	2.35E-01	−1.16E-01	7.06E-03	0.122
0.03	10 ⁸	1.30E-03	1.36E-01	−1.02E-01	7.83E-03	0.182	3.61E-04	2.06E-01	−1.15E-01	7.25E-03	0.180
0.03	10 ⁹	1.92E-03	6.25E-02	−9.61E-02	7.93E-03	0.071	8.03E-04	1.40E-01	−1.11E-01	7.51E-03	0.068
0.03	10 ¹⁰	2.04E-03	3.35E-02	−9.28E-02	7.84E-03	0.063	8.45E-04	1.15E-01	−1.08E-01	7.44E-03	0.063

Note. — Coefficients of best-fit third-order polynomials for the extinction curves in Figure 12 for *HST* NICMOS filter pairs. The difference of the estimated extinction and the true extinction is fitted to a function $[A_Y^{est} - A_Y] = c_0 + c_1[A_Y^{est}] + c_2[A_Y^{est}]^2 + c_3[A_Y^{est}]^3$; $\sigma(A^{est})$ is the average of the standard deviations of $A_Y^{est} - A_Y$ values.

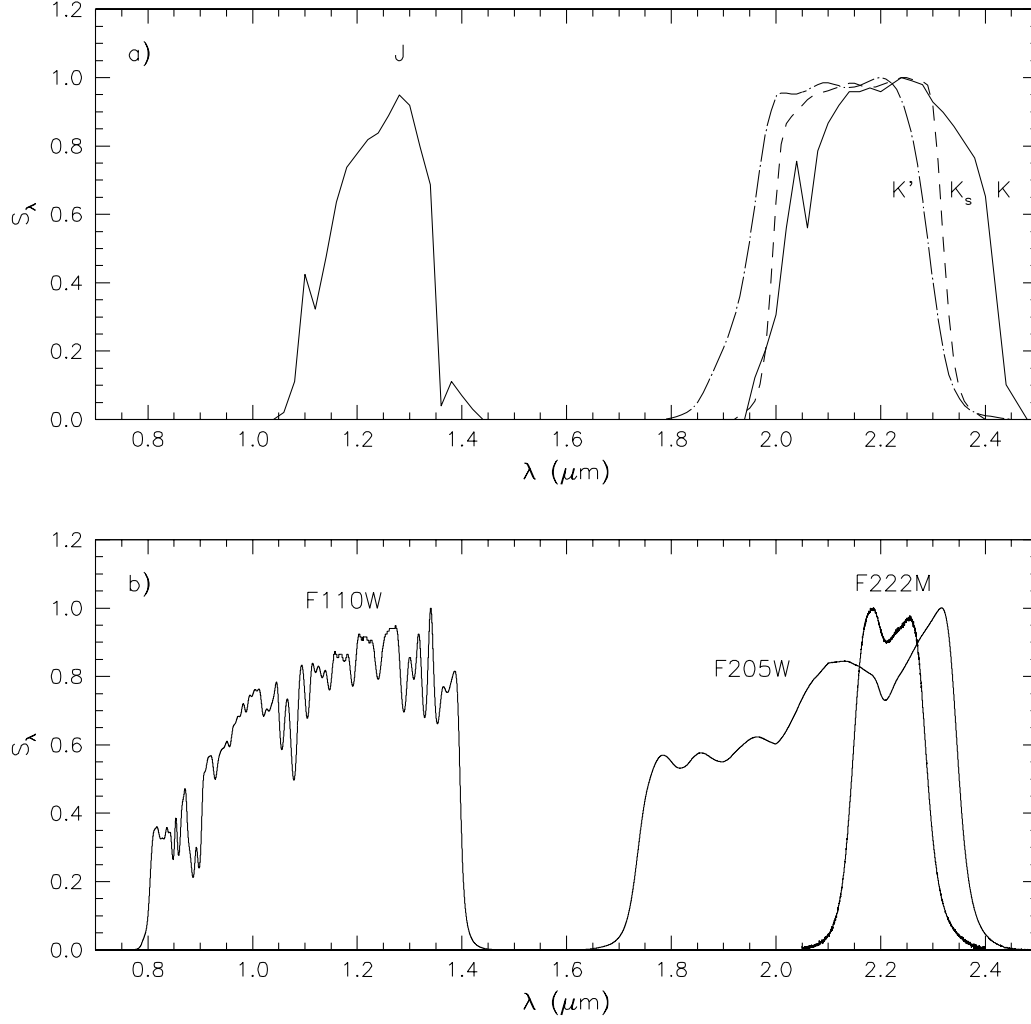


Fig. 1.— Transmission functions (S_λ) of the filters considered in the present work. The S_λ values are scaled such that their maximums occur at 1.

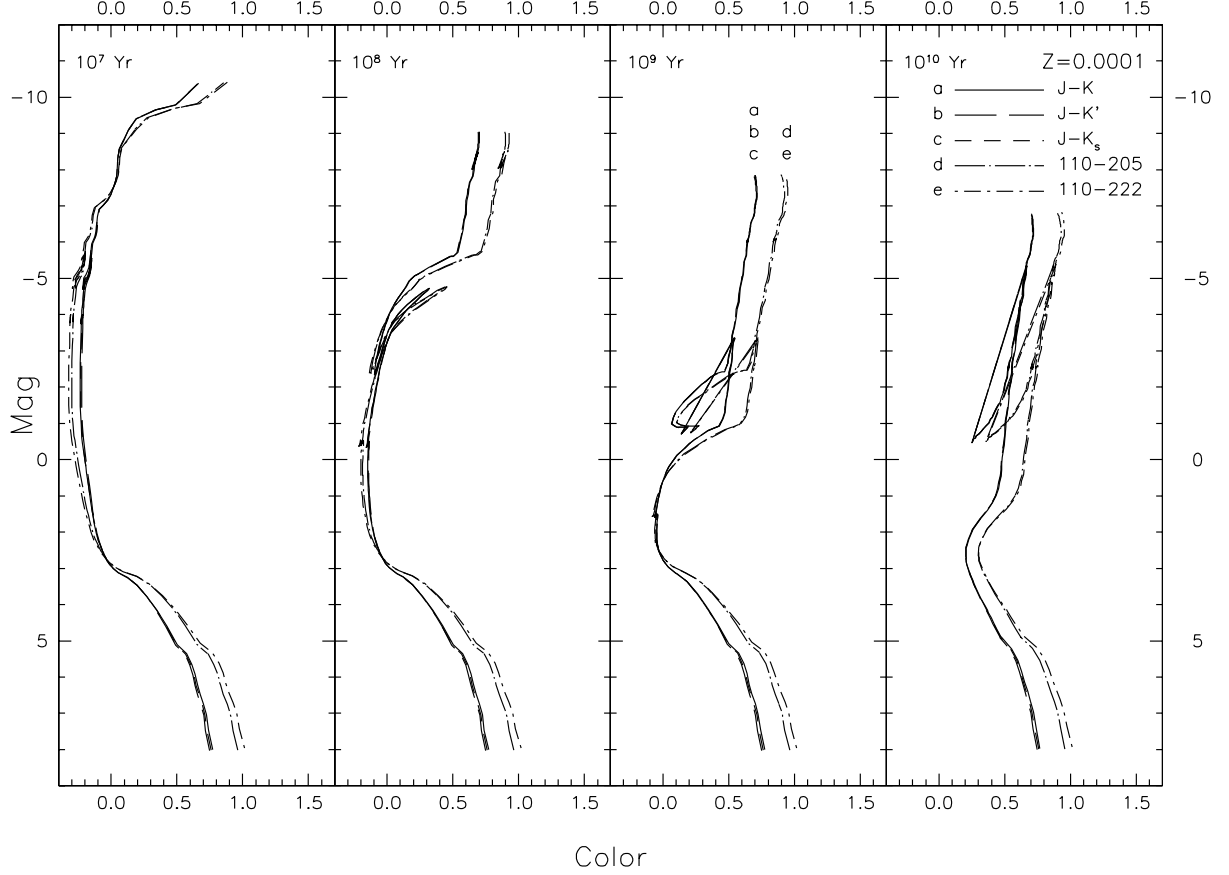


Fig. 2.— Isochrones of the $Z = 0.0001$ model for $J - K$ vs. K (solidline), $J - K'$ vs. K' (long-dashedline), $J - K_s$ vs. K_s (short-dashedline), F110W-F205W vs. F205W (long-dash-dottedline), and F110W-F222M vs. F222M (short-dash-dottedline) in the Vega magnitude system. The three atmospheric filters nearly coincide at the bright end. Only the data points that have $\log T_{eff} \geq 3500$ K and $\log g \geq 0$ are plotted.

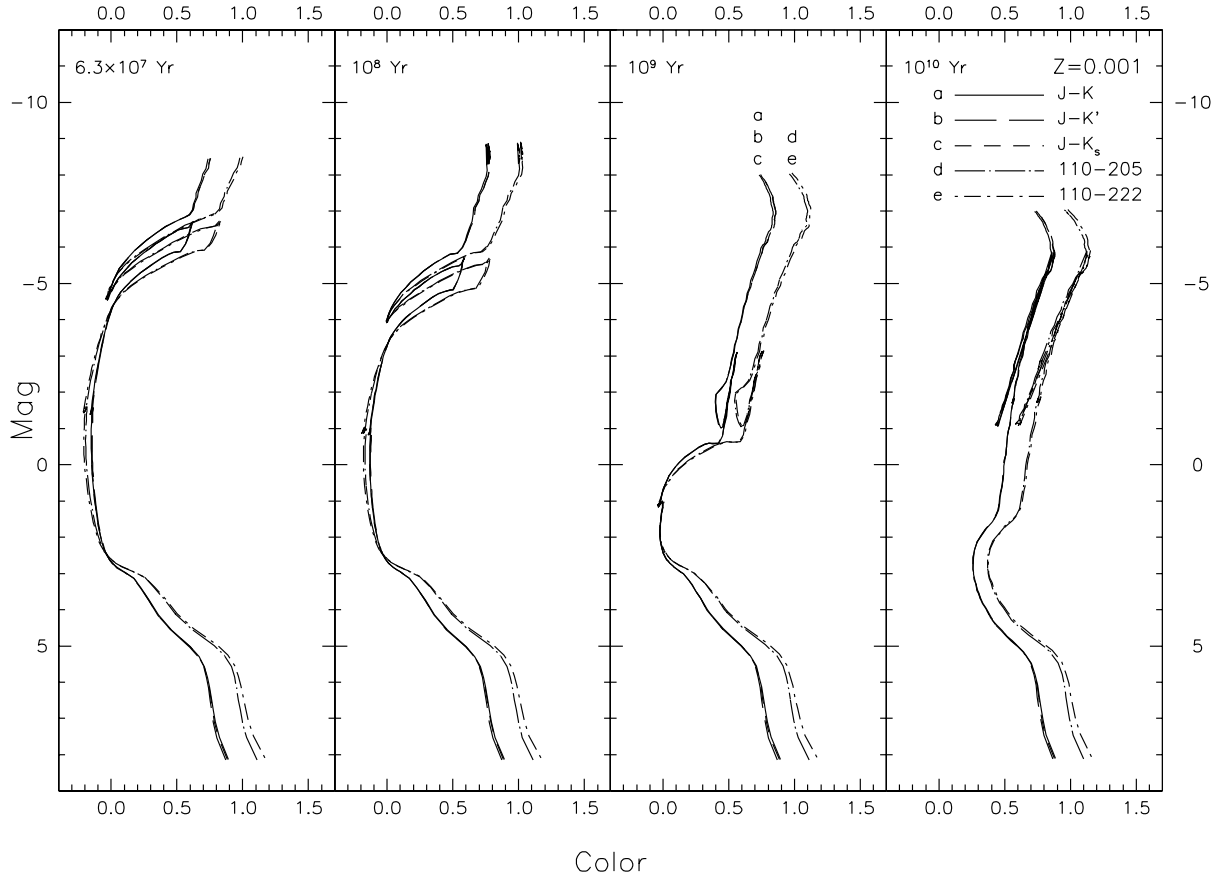


Fig. 3.— Same as Figure 2, but for the $Z = 0.001$ model. Isochrones for K' and K_s are indistinguishable.

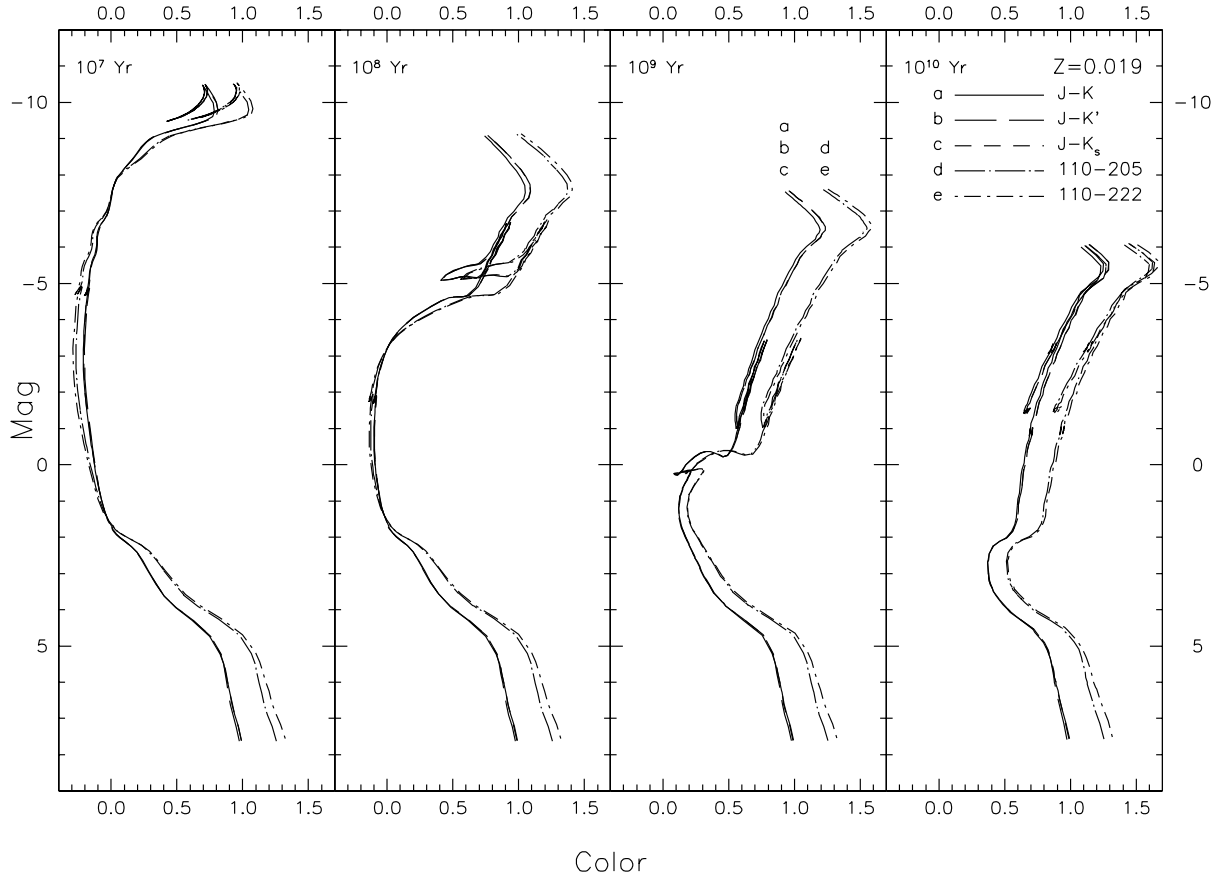


Fig. 4.— Same as Figure 2, but for the $Z = 0.019$ model. Isochrones for K' and K_s are indistinguishable.

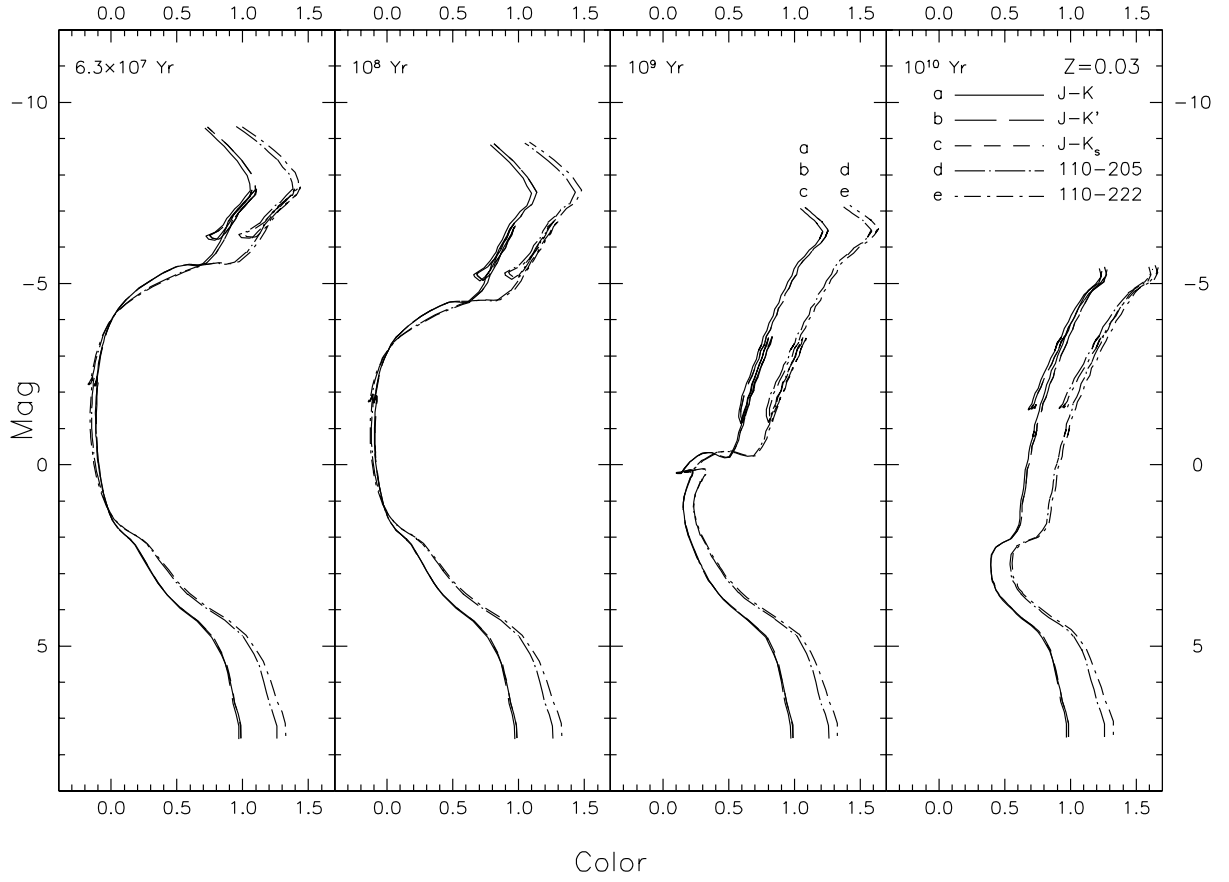


Fig. 5.— Same as Figure 2, but for the $Z = 0.03$ model. Isochrones for K' and K_s are indistinguishable.

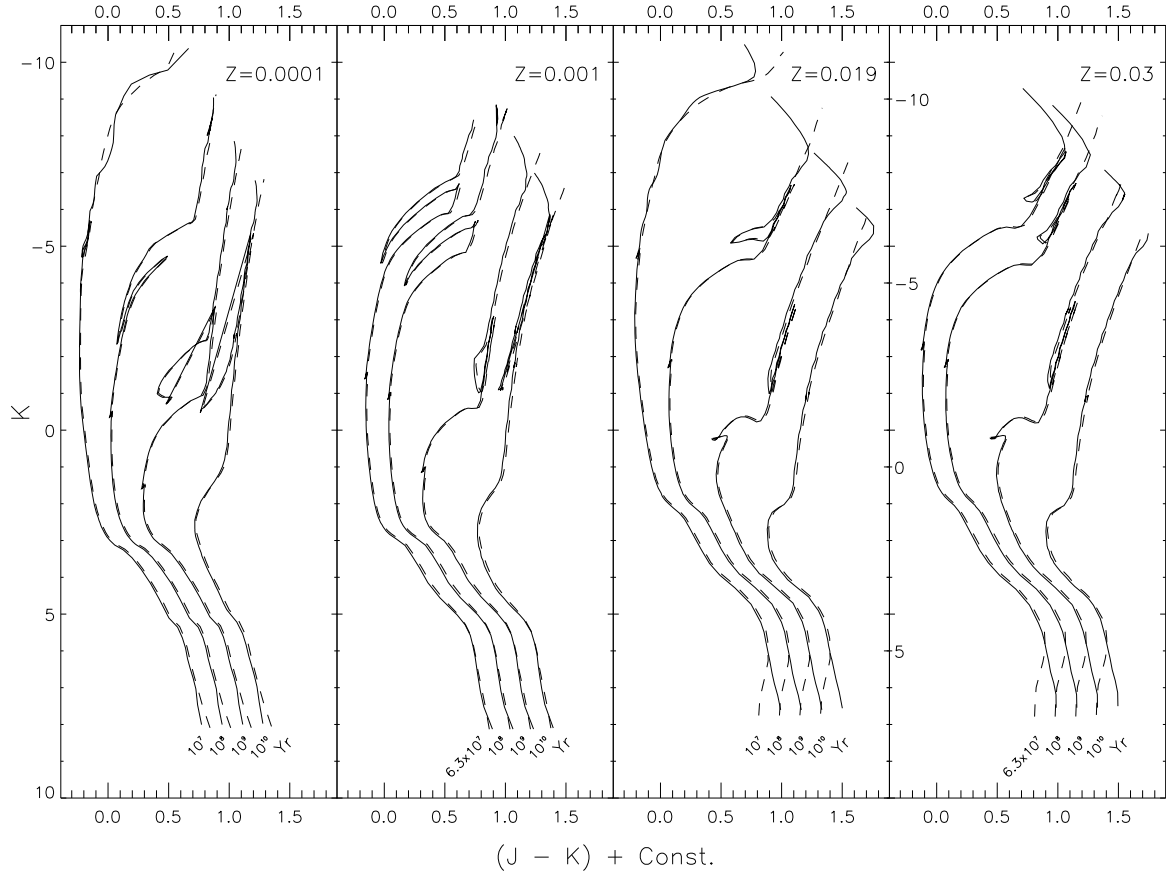


Fig. 6.— Plot of $J - K$ vs. K isochrones calculated in the present study (*solidlines*) and those by Girardi et al. (2002; *dashedlines*). Only data points that have $\log T_{eff} \geq 3500$ K and $\log g \geq 0$ are plotted.

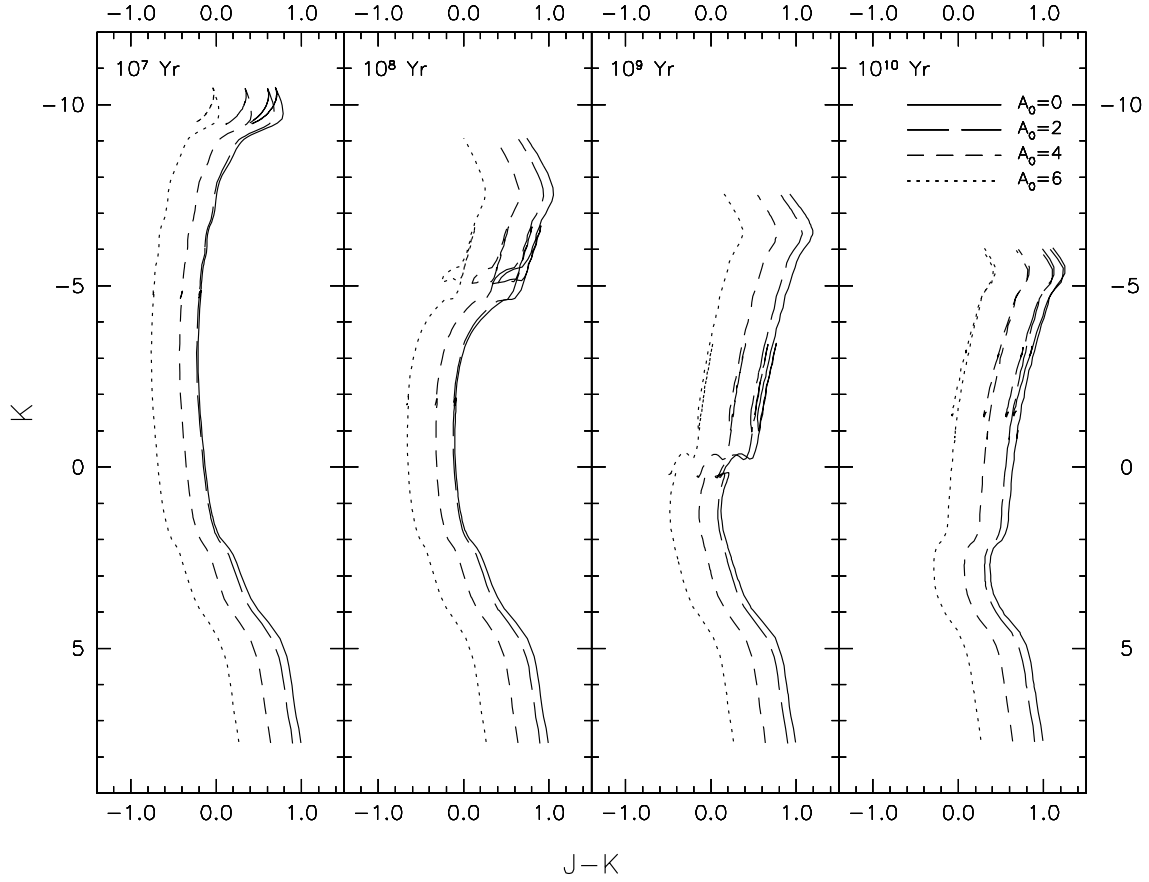


Fig. 7.— Dereddened $J-K$ vs. K isochrones of the $Z = 0.019$ model with $A_0=0$ (*solidline*), $A_0=2$ (*longdashedline*), $A_0=4$ (*shortdashedline*), and $A_0=6$ (*dottedline*). The isochrones are dereddened by an amount $A_0(\lambda_c/\lambda_0)^{-1.66}$. Only data points that have $\log T_{eff} \geq 3500$ K and $\log g \geq 0$ are plotted.

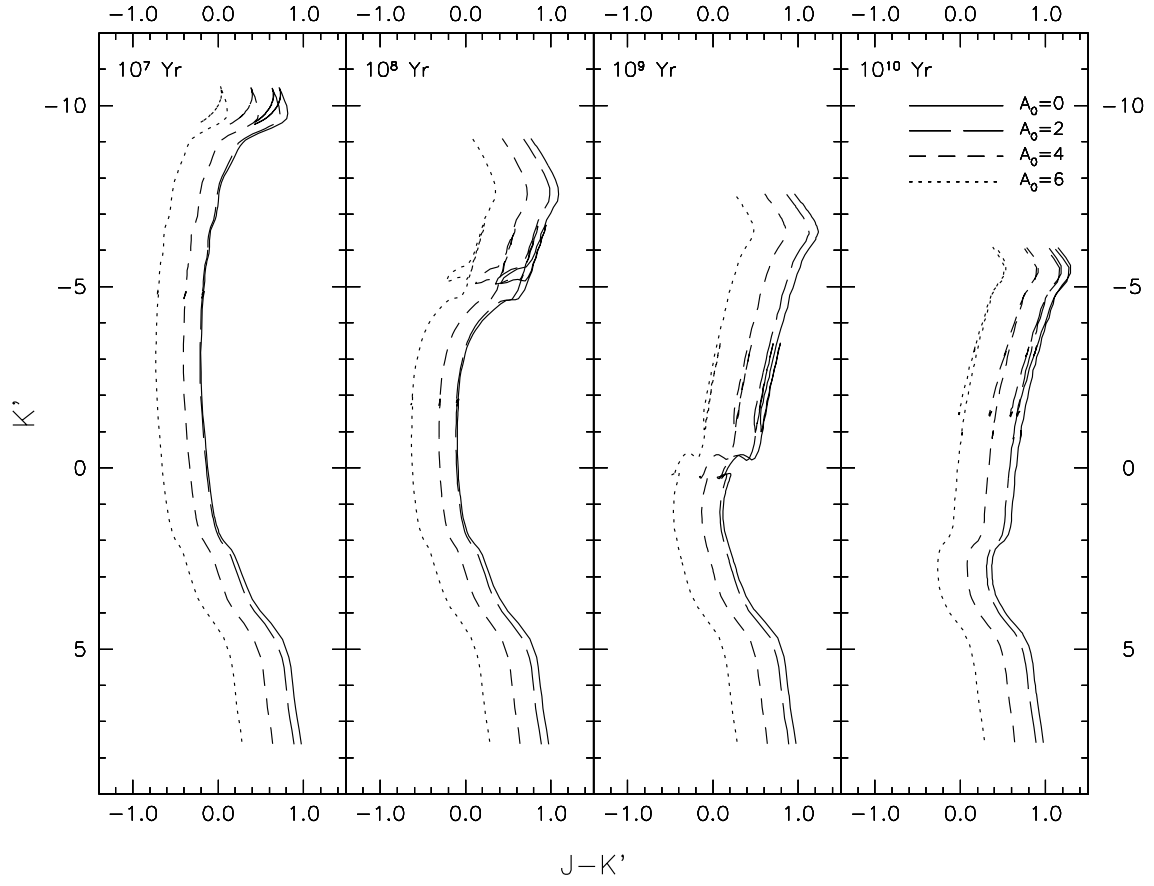


Fig. 8.— Same as Figure 7, but for $J - K'$ vs. K' .

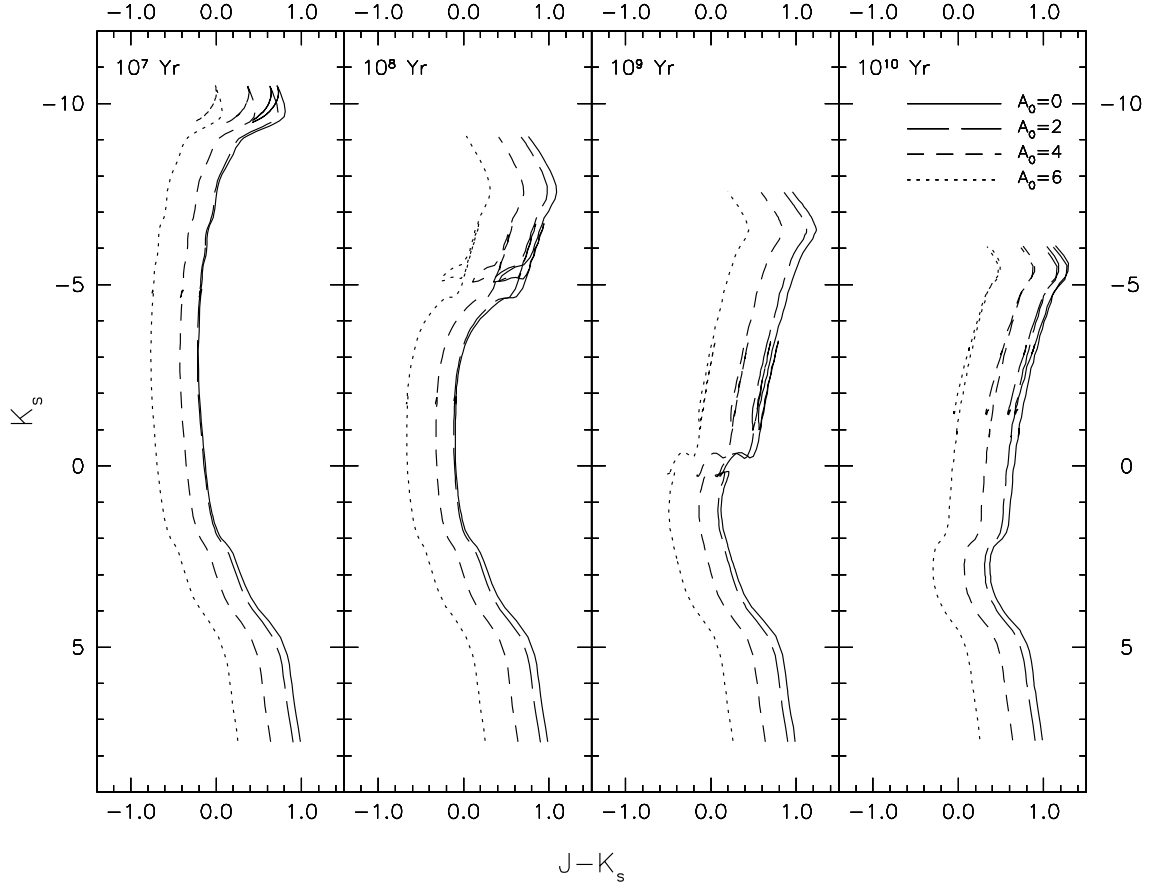


Fig. 9.— Same as Figure 7, but for $J - K_s$ vs. K_s .

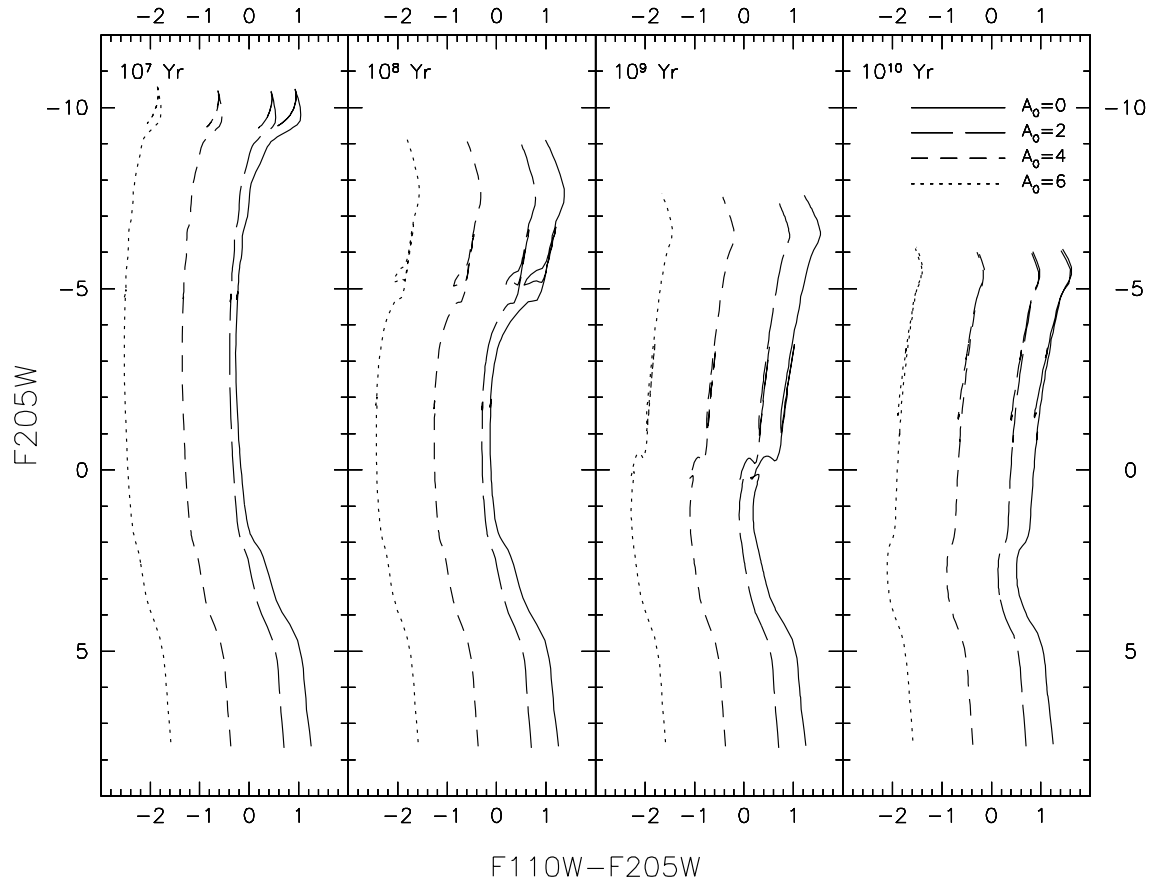


Fig. 10.— Same as Figure 7, but for F110W–F205W vs. F205W.

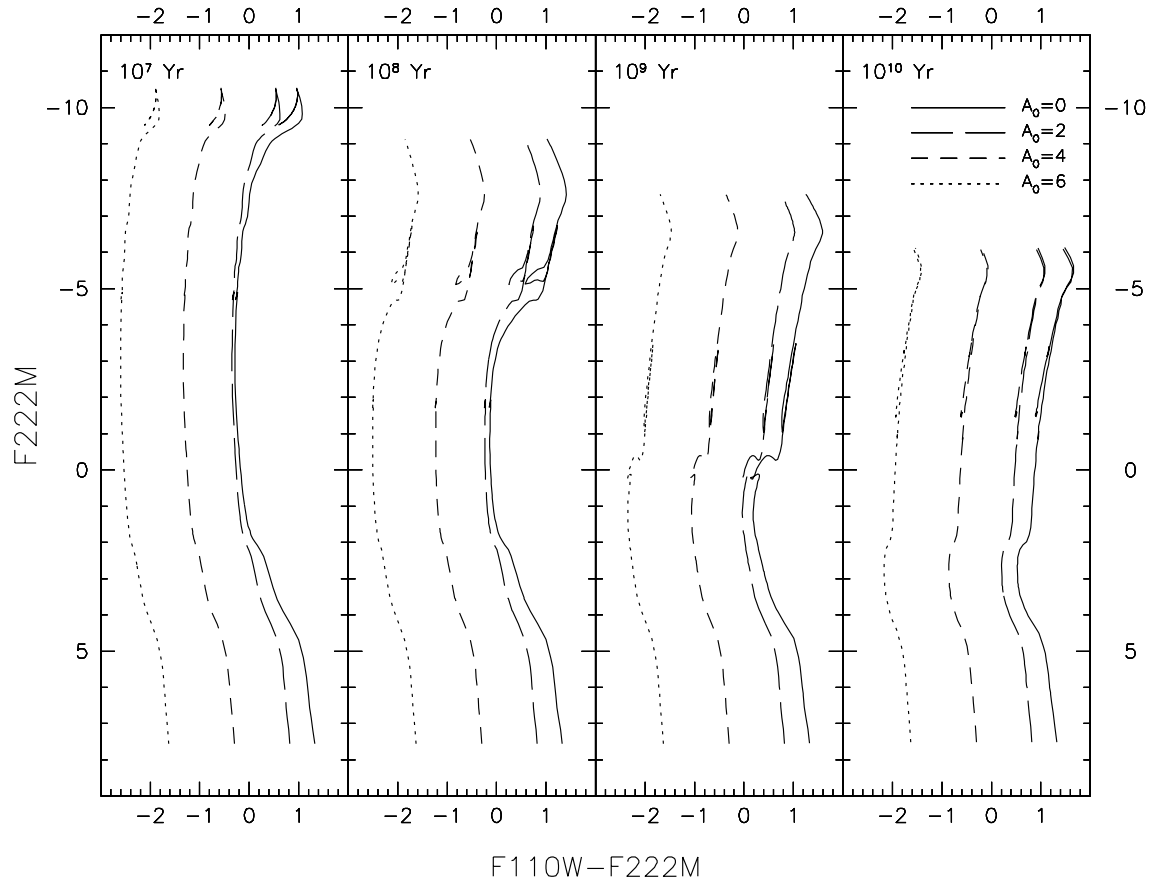


Fig. 11.— Same as Figure 7, but for $F110W-F222M$ vs. $F222M$.

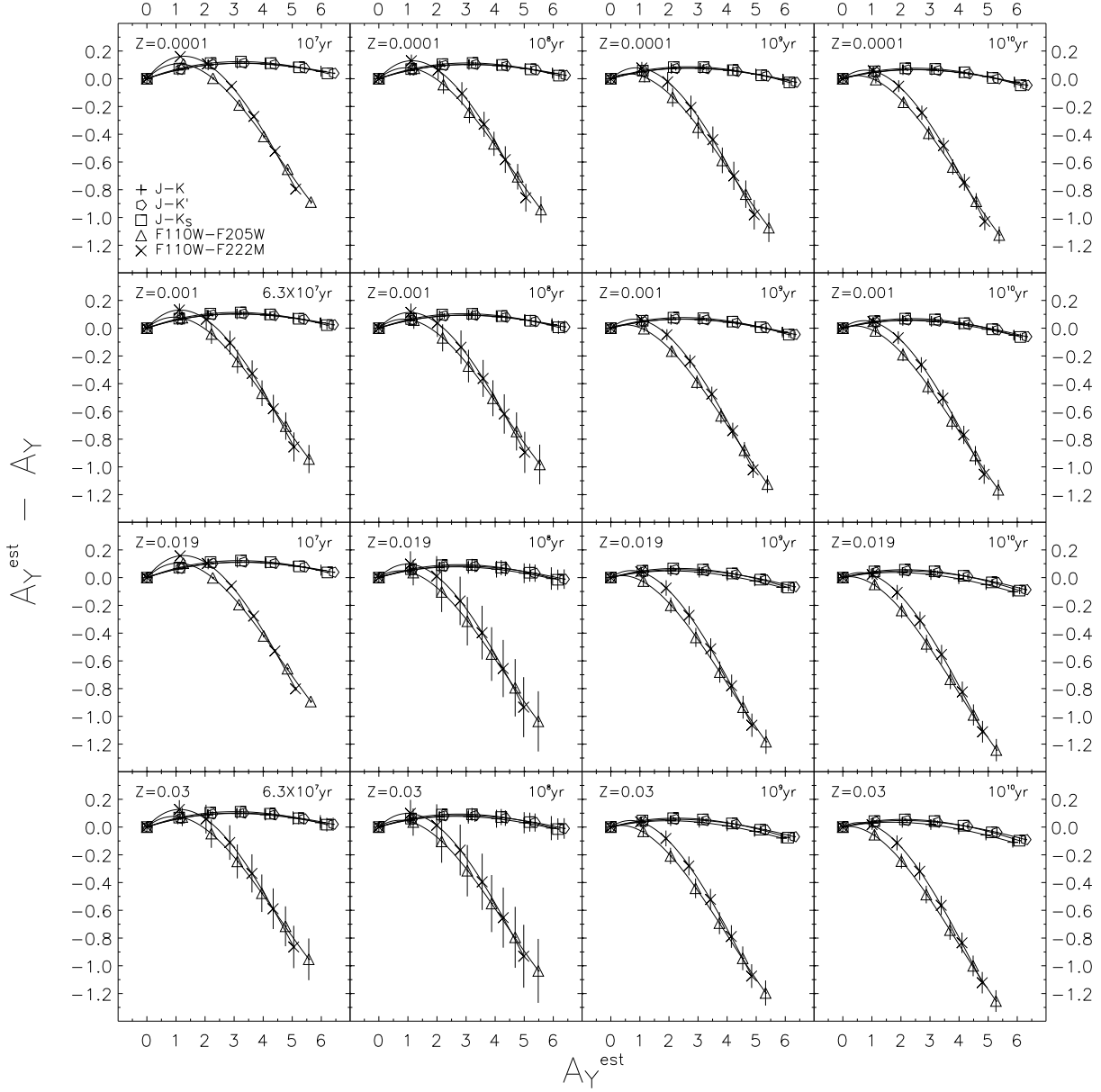


Fig. 12.— Difference between the extinction values that are estimated by eq. (2) using the colors from our reddened isochrones and the actual extinction values. A constant value of 1.59 is used for α in eq. (2). The extinction of each isochrone has been estimated with the mean color (for A_Y^{est}) and the mean magnitude (for A_Y) of the reddened isochrone data points whose intrinsic K -band magnitudes are between -6 and 0 mag. The error bar represents the standard deviation of $A_Y^{\text{est}} - A_Y$ values.

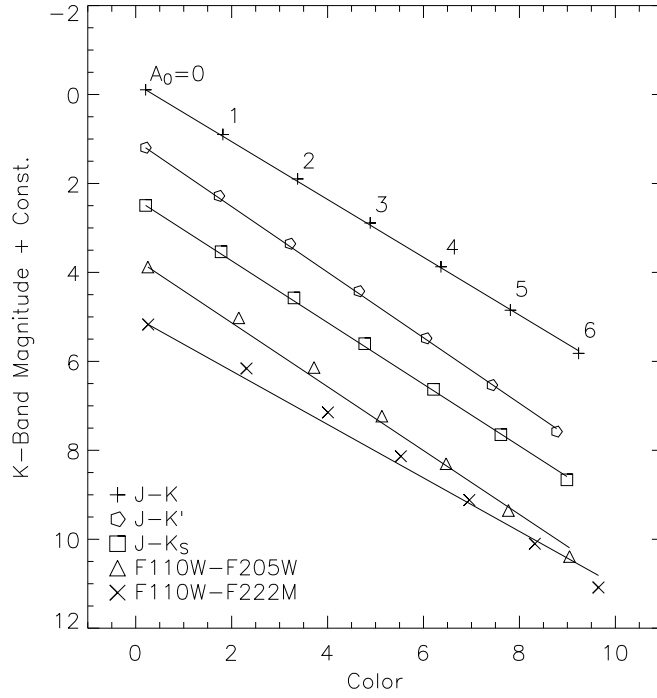


Fig. 13.— Reddened magnitudes of K -band filters and reddened colors for the $Z = 0.019$ and age = 10^9 yr isochrone data point whose intrinsic K magnitude is 0. Also shown are the best-fit straight lines that go through the data point for $A_\lambda = 0$ for each filter pair.

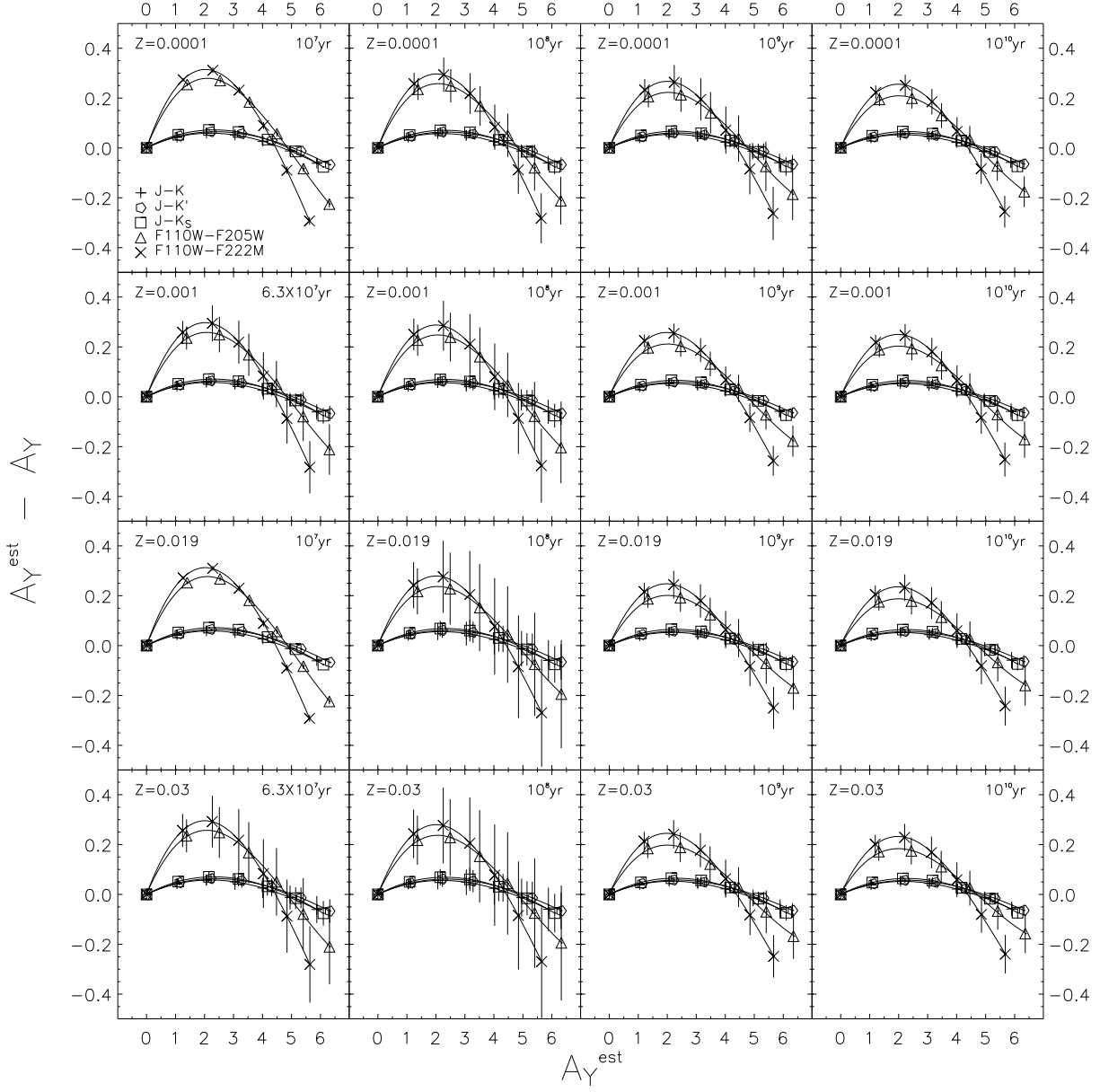


Fig. 14.— Same as Figure 12, but using α_{eff} for eq. (2).

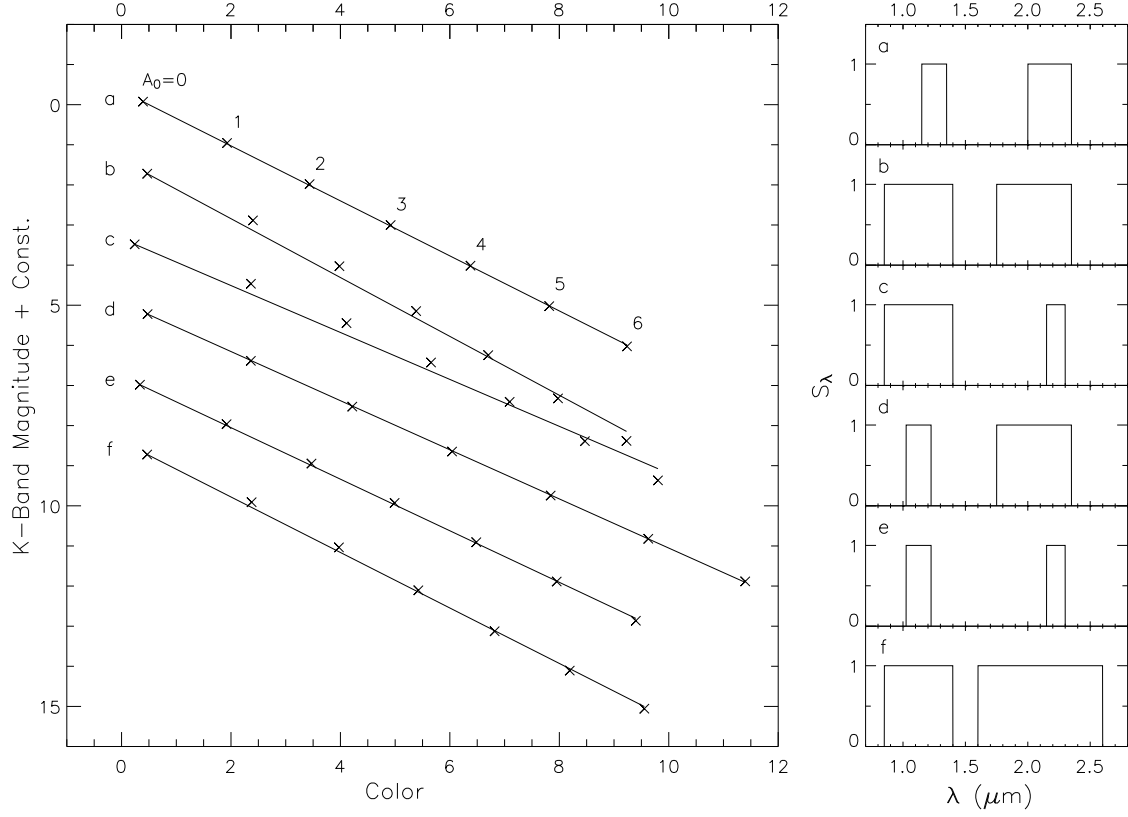


Fig. 15.— Reddened magnitudes and colors (*crosses*) for the $Z = 0.019$ and age = 10^9 yr isochrone data point whose intrinsic K magnitude is 0, for six imaginary filter pairs whose transmission functions are shown in the right panel. Also shown are the best-fit straight lines that go through the data point for $A_\lambda = 0$ for each filter pair.